Inverse Problems 8 (1992) 645–665. Printed in the UK

Numerical performance of layer stripping algorithms for two-dimensional inverse scattering problems

Andrew E Yagle and Poovendran Raadhakrishnan

Department of Electrical Engineering and Computer Science, University of Michigan, Ann Arbor, MI 48109-2122, USA

Received 29 August 1991

Abstract. Numerical results of implementing a two-dimensional layer stripping algorithm to solve the two-dimensional Schrödinger equation inverse potential problem are presented and discussed. This is the first exact (all multiple scattering and diffraction effects are included) numerical solution of a multi-dimensional Schrödinger equation inverse potential problem, excluding optimization-based approaches. The results are as follows: (1) the layer stripping algorithm successfully reconstructed the potential from scattering data measured on a plane (as it would be in many applications); (2) the algorithm avoids multiple scattering errors present in Born approximation reconstructions; and (3) the algorithm is insensitive to small amounts of noise in the scattering data. Simplifications of layer stripping and invariant imbedding algorithms under the Born approximation are also discussed.

1. Introduction

The inverse scattering problem for the Schrödinger equation in two dimensions with a time-independent, local, non-circularly symmetric potential has many applications. Two of these applications are as follows: (1) reconstruction of a three-dimensional (3D) acoustic medium with density and wave speed varying in two dimensions (2D), from surface measurements of the steady-state medium displacement response to a harmonic line source [1]; and (2) reconstruction of a 3D electrical medium with resistivity varying in 2D from surface measurements of the potential resulting from a line DC current source [2]. Both of these applications are quickly reviewed below in section 2.1.

Two major approaches for obtaining exact solutions of the 2D Schrödinger equation inverse potential problem have been proposed. The first is the 2D version of the Gel'fand–Levitan and Marchenko integral equation methods [3]. The other is the 2D version of the layer stripping differential methods [4]. Here 'exact' means that all diffraction and multiple scattering effects are included in the mathematical solution; errors in the solution will arise solely due to purely numerical effects such as discretization and roundoff. Hence all methods based on the Born (single-scattering) approximation are excluded here, since such methods, and their modifications, do not take into account *all* multiple scattering effects. In section 2.4 we discuss how the Born approximation applies to the algorithm of [4]. No numerical implementation of the methods of either [3] or [4] has previously been reported.

0266-5611/92/040645+21$04.50

This paper presents the results of the first numerical implementation of the 2D version of the layer-stripping algorithm of [4]. It is thus the first *exact* (as defined above) numerical solution of a multi-dimensional Schrödinger equation inverse potential problem. Note that optimization-based approaches minimize (or maximize) some criterion; thus they are not in the spirit of the approach considered here. Although only reconstruction of the Schrödinger scattering potential is considered here, direct application to specific inverse scattering problems, as in [1] and [2], would be possible.

This paper is organized as follows. In section 2 the 2D Schrödinger equation inverse potential problem is formulated, two applications are noted, the layer stripping algorithm of [4] is reviewed, details of its numerical implementation are discussed, and its simplification under the Born approximation is discussed. In section 3 the invariant imbedding algorithm of [5] used to generate the scattering data is reviewed, and details of its numerical implementation are discussed. We also discuss its simplification under the Born approximation, and show analytically that the Born-simplified layer stripping algorithm successfully inverts the Born-simplified invariant imbedding algorithm scattering data. Although the latter result is new, it is intended primarily to give some feel for the algorithms of [4] and [5].

Section 4 summarizes the numerical results, and presents some illustrative examples. Issues illustrated include: (1) errors in reconstructed potentials using the Born approximation, which are eliminated using the 'exact' layer stripping algorithm; (2) effects on reconstructed potentials of various amounts of noise in the data; (3) effects on reconstructed potentials of regularization of transverse derivatives in the layer stripping algorithm; and (4) effects of choosing various discretization lengths in the layer stripping algorithm. Section 5 concludes with a summary.

2. Two-dimensional layer stripping algorithm

2.1. Problem formulation and applications

The 2D inverse scattering problem considered in this paper is as follows. The problem is defined in 2D (x, z) space, where x is lateral position and z is depth, increasing downward from the surface $z = 0$. The wavefield $\hat{p}(x, z, k)$ satisfies the 2D Schrödinger equation

$$\left(\frac{\partial^2}{\partial x^2} + \frac{\partial^2}{\partial z^2} + k^2 - V(x, z)\right) \hat{p}(x, z, k) = 0 \tag{2.1}$$

where the potential $V(x, z)$ is real-valued, smooth, and has support in z in the interval $0 < z < L$. It is also assumed that $V(x, z)$ does not induce bound states; a sufficient condition for this is for $V(x, z)$ to be non-negative.

The medium is probed by an impulsive plane wave e^{-ikz}, which passes through the surface $z = 0$ at time $t = 0$ and induces scattering by $V(x, z)$ for $t > 0$. The scattering data consists of measurements of the wavefield $\hat{p}(x, z^*, k)$ and its gradient $\partial\hat{p}(x, z^*, k)/\partial z$ for some z^* in the homogeneous half-space $z \geqslant 0$. For convenience, we assume measurements are taken at the surface $z^* = 0$, as they would be in the applications to follow. The inverse scattering experiment is illustrated in figure 1.

We now quickly review two applications of this problem. First, consider the problem of reconstructing a 3D inhomogeneous acoustic medium whose density $\rho(x, z)$

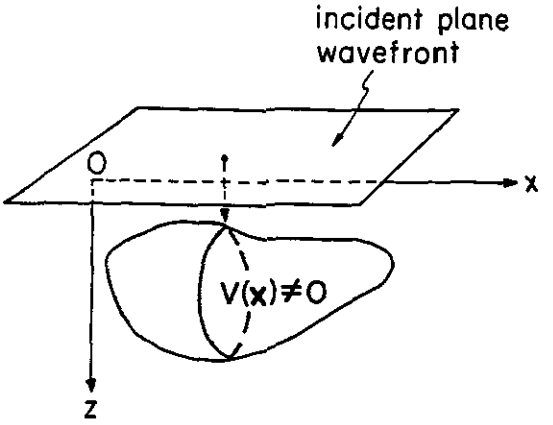

Figure 1. The 2D inverse scattering problem.

and wave speed $c(x,z)$ are smooth functions of depth z and lateral position x. The medium is bounded by a free (pressure-release) surface $z = 0$. The density ρ_0 and wave speed c_0 for $z < 0$ and $z \to \infty$ are known. The medium is probed with cylindrical harmonic waves, at two frequencies ω_1 and ω_2, from a harmonic line source extending along the x-axis, and the sinusoidal steady-state vertical acceleration $\hat{a}(x,y,z=0;\omega_i)$ of the medium at the free surface $z = 0$ is measured. The goal is to reconstruct $\rho(x,z)$ and $c(x,z)$ from the measurements $\hat{a}(x,y,z=0;\omega_i)$, $i = 1,2$.

This problem can be formulated as a 2D Schrödinger equation inverse potential problem by Fourier transforming the basic acoustic equations with respect to time and the other lateral variable y. Details are given in both [1] and [4]. Here we merely note that in the Schrödinger equation (2.1) the wavefield $\hat{p}(x,z,k)$ is pressure divided by $\rho(x,z)^{1/2}$, the wavenumber $k^2 = \omega_i^2/c_0^2 - k_y^2$, and the potential $V(x,z;\omega_i)$ is

$$V(x,z;\omega_i) = \left(\frac{\omega_i^2}{c_0^2}\right)\left(1 - \frac{c_0^2}{c(x,z)^2}\right) + \rho(x,z)^{1/2}\nabla^2(\rho(x,z)^{-1/2}). \tag{2.2}$$

It is clear that performing this experiment for two different frequencies $\omega_i, i = 1,2$ will allow $\rho(x,z)$ and $c(x,z)$ to be computed from (2.2). The wavefield is zero at the free surface $z = 0$; its gradient is the medium acceleration $\rho(x,0)^{1/2}\hat{a}(x,y,z = 0;\omega_i)$, $i = 1,2$.

The second application is the inverse resistivity problem of reconstructing a 3D inhomogeneous electrical medium whose resistivity $\rho(x,z)$ is a smooth function of x and z over a bounded region. The medium is probed with current from a line DC current source extending along the x-axis, and the electrical potential $v(x,y,z=0)$ induced on the surface $z = 0$, assumed to be a perfect insulator, is measured. The goal is to reconstruct the resistivity $\rho(x,z)$ from the measurements of electrical potential $v(x,y,z=0)$. Note that for both applications, the response to a *line* source may be found by superposition of the responses due to *point* sources along the x-axis.

This problem can be formulated as a 2D Schrödinger equation inverse potential problem by Fourier transforming Ohm's and Kirchoff's current laws with respect to the other lateral variable y. Details are given in [5]. Here we merely note that in the Schrödinger equation (2.1) the wavefield $\hat{p}(x,z,k)$ is now the inverse Laplace

transform of the Fourier transform of electrical potential divided by $\rho(x,z)^{1/2}$, and the scattering potential $V(x,z) = \rho(x,z)^{1/2}\nabla^2(\rho(x,z)^{-1/2})$.

2.2. *The 2D layer stripping algorithm*

The layer stripping algorithm for solving the 2D Schrödinger equation inverse potential problem is derived as follows [4]. Taking the inverse Fourier transform of (2.1) with respect to k yields

$$\left(\frac{\partial^2}{\partial x^2} + \frac{\partial^2}{\partial z^2} - \frac{\partial^2}{\partial t^2} - V(x,z)\right)\check{p}(x,z,t) = 0 \tag{2.3}$$

where

$$\check{p}(x,z,t) = \frac{1}{2\pi}\int_{-\infty}^{\infty} \hat{p}(x,z,k)\mathrm{e}^{ikt}\,\mathrm{d}k. \tag{2.4}$$

Equation (2.3) can be written as the coupled system

$$\left(\frac{\partial}{\partial z} + \frac{\partial}{\partial t}\right)\check{p}(x,z,t) = \check{q}(x,z,t) \tag{2.5a}$$

$$\left(\frac{\partial}{\partial z} - \frac{\partial}{\partial t}\right)\check{q}(x,z,t) = \left(V(x,z) - \frac{\partial^2}{\partial x^2}\right)\check{p}(x,z,t) \tag{2.5b}$$

From causality and the form of (2.5a), $\check{p}(x,z,t)$ and $\check{q}(x,z,t)$ have the forms

$$\check{p}(x,z,t) = \delta(t-z) + \tilde{p}(x,z,t)1(t-z) \tag{2.6a}$$

$$\check{q}(x,z,t) = \tilde{q}(x,z,t)1(t-z) \tag{2.6b}$$

where $\tilde{p}$ and $\tilde{q}$ are the smooth parts of $\check{p}$ and $\check{q}$, respectively, and $1(\ )$ is the unit step or Heaviside function.

Inserting (2.6) in (2.5) and equating coefficients of $\delta(t-z)$ (propagation of singularities argument) yields

$$\left(\frac{\partial}{\partial z} + \frac{\partial}{\partial t}\right)\tilde{p}(x,z,t) = \tilde{q}(x,z,t) \tag{2.7a}$$

$$\left(\frac{\partial}{\partial z} - \frac{\partial}{\partial t}\right)\tilde{q}(x,z,t) = \left(V(x,z) - \frac{\partial^2}{\partial x^2}\right)\tilde{p}(x,z,t) \tag{2.7b}$$

$$V(x,z) = -2\tilde{q}(x,z,t = z^+). \tag{2.7c}$$

Equations (2.7) constitute the *basic 2D layer stripping equations*: starting with measured $\tilde{p}(x,0,t)$ and $\tilde{q}(x,0,t)$ (the gradient of the wavefield is required for the latter), propagate (2.7) recursively in increasing depth z, reconstructing $V(x,z)$ as the algorithm proceeds. The coupled equations (2.7a) and (2.7b) include *all* multiple scattering and diffraction effects, since they are equivalent to the Schrödinger equation (2.1) in the time domain. The potential may be reconstructed using (2.7c) since

(2.7) is implemented at the wave front $t = z$; by time causality there has been no time for multiple scattering to occur yet.

Some advantages of using layer stripping algorithms are as follows.

(i) Only backscattered data from one direction of probing is required. Integral equation methods [3] require the scattering amplitude, which is the far-field response in *all* directions to an incident impulsive plane wave in *each* possible direction. In the applications noted above, this is unrealistic; it also runs the risk of inconsistent data.

(ii) The amount of computation required is much less than the amount required to solve the integral equations of [3]. The layer stripping algorithm can be viewed as a fast algorithm solution of these integral equations which exploits the Hankel structure in the kernel of the generalized Marchenko integral equation of [3].

(iii) *All* multiple scattering and diffraction effects are included, unlike methods such as distorted-wave Born approximation which only account for some of these effects.

Two disadvantages of layer stripping algorithms are as follows.

(i) It is not clear how to incorporate the effects of bound states (roughly, square-integrable solutions to the Schrödinger equation with negative energy); unlike the approach of [3].

(ii) The lateral derivative $\partial^2/\partial x^2$ in (2.7*b*) can be expected to induce numerical instability.

2.3. *Numerical implementation of the* 2D *layer stripping algorithm*

The second disadvantage can be removed as follows. Take the Fourier transform of (2.7) with respect to x. The result is

$$\left(\frac{\partial}{\partial z} + \frac{\partial}{\partial t}\right) p(z, t, k_x) = q(z, t, k_x) \tag{2.8a}$$

$$\left(\frac{\partial}{\partial z} - \frac{\partial}{\partial t}\right) q(z, t, k_x) = k_x^2 p(z, t, k_x) + \hat{V}(z, k_x) * p(z, t, k_x) \tag{2.8b}$$

$$\hat{V}(z, k_x) = -2q(z, t = z^+, k_x) \tag{2.8c}$$

where $*$ denotes convolution in k_x

$$p(z, t, k_x) = \int_{-\infty}^{\infty} \tilde{p}(x, z, t) e^{-ik_x x} dx \tag{2.9}$$

and $q(z, t, k_x)$ and $\hat{V}(z, k_x)$ are defined similarly.

The multiplication by k_x^2 in (2.8*b*) will induce numerical instability. This may be avoided by replacing the multiplication by k_x^2 in (2.8*b*) with multiplication by the clipped filter

$$H(k_x) = \begin{cases} k_x^2 & \text{if } |k_x| < K \\ 0 & \text{otherwise} \end{cases} \tag{2.10}$$

for some cutoff wavenumber K. This is reminiscent of the clipped filter used in the filtered back-projection procedure for inverting the Radon transform. In practice, the

discontinuities in (2.10) at $|k_x| = K$ would be replaced by a smooth window to zero; a Hanning (raised cosine) window was used in the numerical simulations presented later.

We now discretize depth $z = n\Delta$ and time $t = j\Delta$ to integer multiples of some discretization length Δ. Since the wave speed in (2.1) is unity, depth and time have the same Δ. Lateral position x would also use the same Δ; but wavenumber $k_x = k\Delta_k$ must use for Δ_k half the reciprocal of the total lateral extent of interest; e.g. if the potential has finite support $-L_x/2 < x < L_x/2$ in x, L_x would be the lateral extent of interest. Note that Δ and Δ_k have reciprocal units.

Using forward difference approximations to the partial derivatives then yields

$$p((n+1)\Delta,(j+1)\Delta,k\Delta_k) = p(n\Delta,j\Delta,k\Delta_k) + q(n\Delta,j\Delta,k\Delta_k)\Delta \tag{2.11a}$$

$$q((n+1)\Delta,(j-1)\Delta,k\Delta_k) = q(n\Delta,j\Delta,k\Delta_k) + H(k\Delta_k)p(n\Delta,j\Delta,k\Delta_k)\Delta + \sum_{m=-\infty}^{\infty} \hat{V}((k-m)\Delta_k)p(n\Delta,j\Delta,m\Delta_k)\Delta\Delta_k \tag{2.11b}$$

$$V((n+1)\Delta,k\Delta_k) = -2q((n+1)\Delta,(n+1)\Delta,k\Delta_k). \tag{2.11c}$$

Equations (2.11) constitute the numerical implementation of the 2D layer stripping algorithm. The update patterns are illustrated in figure 2; note that by time causality $p(z,t,k_x)$ and $q(z,t,k_x)$ are zero for $t < z$.

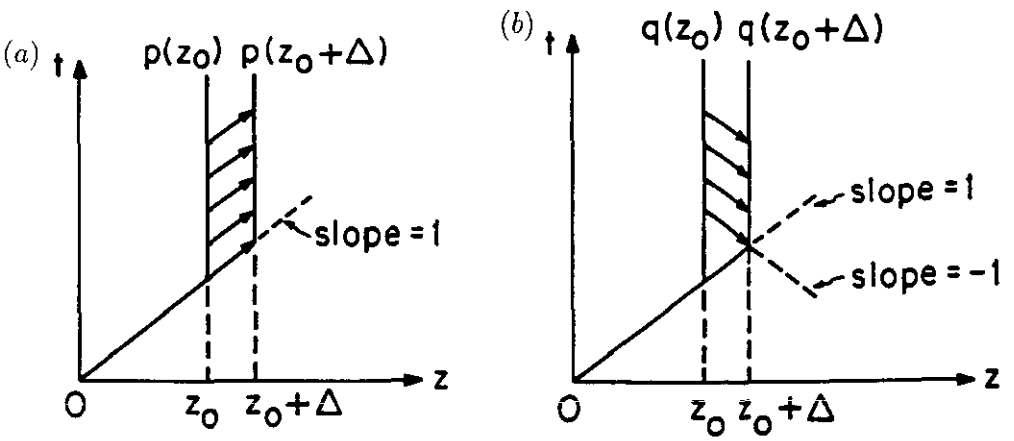

Figure 2. Update patterns for (*a*) $p(z,t,k_x)$ and (*b*) $q(z,t,k_x)$.

Cheney [6] has shown that the modification (2.10) stabilizes the layer stripping algorithm (2.11), in the following sense. Define the norm

$$||f(k_x,t)|| = \sup_{t>0} \int_{-\infty}^{\infty} |f(k_x,t)|\,dk_x. \tag{2.12}$$

Input two different sets of bounded initial data $p_i(k_x,0,t), q_i(k_x,0,t), i = 1,2$ into the discretized algorithm (2.11), resulting in two different reconstructed potentials

$\hat{V}_i(k_x, z)$, $i = 1, 2$. Let $||p_i(k_x, 0, t)|| < K'$ and $||q_i(k_x, 0, t)|| < K'$ for some K'. Then for $z = n\Delta$ we have

$$\sup_{k_x}[\hat{V}_1(k_x, z) - \hat{V}_2(k_x, z)]$$
$$\leqslant K_1(z)||p_1(k_x, 0, t) - p_2(k_x, 0, t)|| + K_2(z)||q_1(k_x, 0, t) - q_2(k_x, 0, t)|| \tag{2.13}$$

where $K_1(z)$ and $K_2(z)$ are polynomials in n, Δ, K, and K'.

The discretized system (2.11) can be implemented as is. However, its spectral properties are worth examining. It might seem as though we can regard the discretized functions $p(n\Delta, j\Delta, k\Delta)$, etc, as merely sampled versions of the continuous functions $p(z, t, k_x)$, etc, provided the latter are bandlimited and sampling is performed above the Nyquist rate. However, the nonlinear product in (2.7*b*) becomes the convolution in k_x in (2.8*b*) and (2.11*b*); the wavenumbers become mixed. Indeed, even if the inverse potential problem is regularized by assuming that $\hat{V}(z, k_x)$ is bandlimited in z and zero for $|k_x| > K$ for some K, it is clear that $p(z, t, k_x)$, etc. will *not* have similar properties. Imposing a bandlimited condition at each recursion will lead to errors, since the missing high wavenumbers will cause errors at low wavenumbers due to the wavenumber mixing. This leads to the question of what the discretized $p(n\Delta, j\Delta, k\Delta_k)$, etc mean, and how the convolutions in k_x should be performed. It should be noted that similar questions arise in integral equation methods.

One possible interpretation is to perform a periodic extension in k of all quantities in (2.11). The period in k should be $1/\Delta_k$; K in (2.10) should then be half this. It is clear by induction that if all quantities at depth $n\Delta$ are periodic in k, then all quantities at depth $(n+1)\Delta$ will also be periodic in k. This has two advantages: (1) the infinite linear convolution becomes a finite cyclic convolution; and (2) the discrete Fourier transform may be used to perform all Fourier transforms. Since periodicity in one Fourier domain is equivalent to discreteness in the other Fourier domain, the problem has effectively been discretized laterally as well as vertically: the quantites propagated in (2.11) are not samples of a bandlimited function, but actual discrete values. As $\Delta_k \to 0$, the situation approaches the continuous problem.

2.4. Born approximation to the layer stripping algorithm

It is worth noting how the Born approximation applies to the layer stripping equations (2.7). The Born approximation is a linearization of the inverse potential problem; the idea is to render the potential to be linearly related to the scattering data. This has been discussed in detail elsewhere; here we merely scale the potential by a small parameter ϵ, expand $\tilde{p}(x, z, t)$, etc. in a Taylor series in ϵ, and discard all terms of order ϵ^2 or smaller. The result is elimination of the product in (2.7*b*); since this is the one nonlinearity in (2.7) its elimination is not surprising. Combining the modified (2.7*a*) and (2.7*b*) and keeping (2.7*c*) results in

$$\left(\frac{\partial^2}{\partial x^2} + \frac{\partial^2}{\partial z^2} - \frac{\partial^2}{\partial t^2}\right)\tilde{q}(x, z, t) = 0 \tag{2.14a}$$

$$V(x, z) = -2\tilde{q}(x, z, t = z^+). \tag{2.14b}$$

We recognize (2.14*a*) as the migration operator relating the wavefield at the surface $z = 0$ to the wavefield on the plane parallel to the surface at depth z, and (2.14*b*) as the imaging operator (gradient) applied to the migrated wavefield. Taking two Fourier transforms of (2.14*a*) with respect to t and x and using (2.4) and (2.9) yields

$$\left(\frac{\partial^2}{\partial z^2} + (k^2 - k_x^2)\right)\bar{q}(k_x, z, k) = 0 \qquad \bar{q}(k_x, z, k) = \mathcal{F}_{t\to k}\mathcal{F}_{x\to k_x}\{\tilde{q}(x, z, t)\} \tag{2.15}$$

a differential equation which has the solution

$$\bar{q}(k_x, z, k) = \bar{q}(k_x, 0, k)\mathrm{e}^{-\mathrm{i}\sqrt{k^2 - k_x^2}z}. \tag{2.16}$$

The operation of the Born approximation to the layer stripping equations is now clear: (1) migrate the wavefield from the surface to depth z; and (2) image the wavefield at depth z to obtain the scattering potential. Note that imaging the potential requires taking the gradient of the wavefield; this is why q, not p, is used. Note also that multiple scattering, which is inherently nonlinear, is neglected in (2.14) and (2.16). The coupling induced by the product term in (2.7) accounts precisely for all multiple scattering. More details about the Born approximation and its relation to layer stripping and integral equation methods is available in [4] and [7].

From the Schrödinger equation (2.1), it is apparent that for large wavenumbers k the potential $V(x, z)$ will be relatively small, and that multiple scattering will be less significant. Indeed, in the limit $k \to \infty$ the Born approximation becomes exact, in that multiple scattering effects become negligible. However, inversion based solely on asymptotically large k is clearly unstable; 'exact' inverse scattering methods use low-wavenumber data as well as high-wavenumber data to stabilize the reconstruction. Also, it is clear that multiple scattering is more significant for small k ($V(x, z)$ is relatively large), so lack of high-wavenumber data makes the use of 'exact' methods even more imperative.

3. Forward problem algorithm

3.1. Invariant imbedding algorithm

The invariant imbedding algorithm of [5] was used to generate the scattering data, to be input into the layer stripping algorithm. We briefly review this algorithm here, following the notation of [5] for convenience. Let k be wavenumber, as in the Schrödinger equation (2.1), $q = k_x$ (lateral wavenumber), $k(q) = \sqrt{k^2 - q^2}$ (vertical wavenumber, as in (2.16)), and p be lateral wavenumber of the incident plane wave (ultimately we are interested in $p = 0$). Then further define $h(z, q) = \hat{V}(z, k_x)$ (scattering potential) and $u(z, q) = \bar{p}(k_x, z, k)$ (wavefield; see (2.15)). A slight problem with the notation of [5] is that the dependence of $u(z, q)$ and $R(c, q, p)$ on k is not explicit.

Finally, define $R(c, q, p)$ as the near-field planar reflection response, in direction q, of the portion of the medium below depth c, to an impulse $\delta(q-p)\mathrm{e}^{-\mathrm{i}k(q)z}/k(p)$, in direction p (recall directions are specified by wavenumbers). Two *inverse* Fourier transforms taking $k \to t$ and $q = k_x \to x$, as in (2.15), transform $\delta(q - p)\mathrm{e}^{-\mathrm{i}k(q)z}$

into the impulsive plane wave $\delta(t - z\cos\theta - x\sin\theta)$, where θ is the angle of incidence (measured from the vertical) defined by $p = k\sin\theta$. Hence $k(p)R(0,q,0)$, computed for each k and then inverse Fourier transformed as in (2.4), is precisely the reflection response to an impulsive plane wave normally incident on the medium.

We sketch through the derivation of the invariant imbedding equations to show the similarities and differences to layer stripping. A Fourier transform of the Schrödinger equation (2.1) taking $x \to q = k_x$ yields (recall $h(z,q) = \hat{V}(z,k_x)$)

$$\left(\frac{\partial^2}{\partial z^2} + k^2(q) - h(z,q)*\right) u(z,q) = 0 \tag{3.1}$$

where $*$ denotes convolution in q and $k^2(q) = k^2 - q^2$. Defining

$$v(z,q) = \frac{1}{2}\left(u(z,q) + \frac{\partial u}{\partial z}\frac{1}{\mathrm{i}k(q)}\right) \qquad w(z,q) = \frac{1}{2}\left(u(z,q) - \frac{\partial u}{\partial z}\frac{1}{\mathrm{i}k(q)}\right) \tag{3.2}$$

it can be shown [5, p 93] that $v(z,q)$ and $w(z,q)$ satisfy the coupled system (compare with (2.8))

$$\frac{\mathrm{d}}{\mathrm{d}z}\begin{bmatrix} v \\ w \end{bmatrix} = \begin{bmatrix} \mathrm{i}k(q)v - (h*(v+w))/(2\mathrm{i}k(q)) \\ -\mathrm{i}k(q)w + (h*(v+w))/(2\mathrm{i}k(q)) \end{bmatrix} \tag{3.3}$$

where all variables are functions of (z,q).

Now *imbed* the system (3.3) as follows. Let $A(z,c,q,p)$ and $B(z,c,q,p)$ satisfy (3.3), initialized with $A(z=c,c,q,p) = \delta(q-p)/k(p)$ and $B(z=L,c,q,p) = 0$ (the latter is a radiation condition; recall $V(x,z)$ has support in $0 < z < L$). Then

$$\begin{aligned} v(z,q) &= kA(z,0,q,p) & w(z,q) &= kB(z,0,q,p) \\ A(c,c,q,p) &= \delta(q-p)/k(p) & R(c,q,p) &= B(c,c,q,p). \end{aligned} \tag{3.4}$$

Furthermore, $\partial A/\partial c$ and $\partial B/\partial c$ also satisfy (3.3), but with initial conditions

$$\frac{\partial A}{\partial c}(c,c,q,p) = -\frac{\partial A}{\partial z}(c,c,q,p) \qquad \frac{\partial B}{\partial c}(L,c,q,p) = 0. \tag{3.5}$$

By superposition, the solution to (3.3) with these initial conditions is [5, p 95]

$$\frac{\partial A}{\partial c}(z,c,q,p) = -\int A(z,c,q,q')k(q')\frac{\partial A}{\partial z}(c,c,q',p)\,\mathrm{d}q' \tag{3.6a}$$

$$\frac{\partial B}{\partial c}(z,c,q,p) = -\int B(z,c,q,q')k(q')\frac{\partial A}{\partial z}(c,c,q',p)\,\mathrm{d}q'. \tag{3.6b}$$

We also have from the last of (3.4)

$$\frac{\mathrm{d}R}{\mathrm{d}c}(c,q,p) = \frac{\mathrm{d}B}{\mathrm{d}c}(c,c,q,p) = \frac{\partial B}{\partial z}(c,c,q,p) + \frac{\partial B}{\partial c}(c,c,q,p). \tag{3.7}$$

Finally, setting $z = c$ in (3.3), substituting into (3.6), and substituting again into (3.7) gives the following *invariant imbedding equation for R(c,q,p)*:

$$\begin{aligned} i\frac{dR}{dc}(c,q,p) &= (k + k(q))R(c,q,p) + h(c,q-p)/(2k(q)k) \\ &+ \iint R(c,q,q')h(c,q'-q'')R(c,q'',p)/2\,dq'\,dq'' \\ &+ \int (h(c,q-q')R(c,q',p)/k(q) + R(c,q,q')h(c,q'-p)/k)/2\,dq' \\ R(L,q,p) &= 0. \end{aligned} \tag{3.8}$$

This is formaula (11*a*) in [5, p 97].

Note that (3.8) is computed recursively in decreasing c, starting at $c = L$ and ending at $c = 0$. This must be done for each p, q, and k (recall that $R(c,q,p)$ also depends on k; this dependence is not shown explicitly in (3.8) since none of the integrations are over k). Having computed $R(0,q,p)$ for all k, i.e. having computed $R(0,q,p,k)$, the inverse Fourier transform (2.4) of $kR(0,q,0,k)$ is precisely the reflection response to an impulsive plane wave normally incident on the medium. This is the scattering data used as input to the layer stripping algorithm.

3.2. Numerical implementation of invariant imbedding algorithm

Despite its apparent complexity, (3.8) can be implemented numerically in a straightforward manner by discretization similar to that used to obtain (2.11) from (2.8). Since (3.8) is already in the wavenumber domain, and the scattering potential $h(z,q)$ is known exactly, no computational instability issues arise. The integrals may be evaluated using the trapezoidal rule, and a backward difference approximation to dR/dc used to propagate (3.8) in *decreasing* c from $c = L$ to $c = 0$.

Once again we assume a periodicity of $1/\Delta$ in the values of all functions of wavenumbers; this corresponds to the discretized functions being actual discrete values, rather than sampled values of bandlimited continuous functions. The infinite integrals in (3.6) and (3.8) become cyclic integrals (computed only over one period), so their evaluation is straightforward. The multiplication by $k + k(q)$ in (3.8) is windowed to zero for values greater than $1/(2\Delta)$, as in (2.10), and then periodically extended.

Note that it is not possible to compute the reflection response for $k = 0$ or $k(q) = 0$, due to the divisions by these in (3.8). The former can be assumed to be zero, since a non-zero DC reflection response would represent *permanent* displacement resulting from the impulsive plane wave! The latter corresponds to incidence at 90 degrees, which would not create a backscattered field in the $+z$ direction. Hence omitting these does not present a problem.

3.3. Born approximation to invariant imbedding algorithm

The invariant imbedding equation (3.8) is suggestive of a 2D version of the Riccati equation familiar in 1D scattering in layered media. The two integral terms correspond to the square term in the 1D Riccati equation. To aid in understanding (3.8), we now apply the Born approximation to (3.8), and show that the Born approximation to the layer stripping algorithm (2.14*b*) and (2.16) reconstructs the potential from the

reflection response generated by the Born approximation to the invariant imbedding equation (3.8).

As in section 2.4, we scale the potential by a small parameter ϵ, expand the wavefield and reflection response in a Taylor series in ϵ, and discard all terms of order ϵ^2 or smaller. The result is elimination of the two integrals of products terms in (3.8), leaving

$$\mathrm{i}\frac{\mathrm{d}R}{\mathrm{d}c}(c,q,p) = (k+k(q))R(c,q,p) + h(c,q-p)/(2k(q)k) \qquad R(L,q,p) = 0. \tag{3.9}$$

Since there is no longer coupling between $R(c,q,p)$ of different p, we can set $p = 0$ (normal incidence) and solve the differential equation (3.9), yielding

$$kR(z,q,k) = -\mathrm{i}\mathrm{e}^{-\mathrm{i}(k(q)+k)z}\int_L^z \frac{\hat{V}(z',q)}{2k(q)}\mathrm{e}^{\mathrm{i}(k(q)+k)z'}\,\mathrm{d}z'. \tag{3.10}$$

The factor of k multiplying $R(z,q,k)$ is present because $k(p)R(z,q,p,k)$ is the Fourier transform of the reflection response to an impulse, as discussed in the second paragraph of section 3.1. Since $p = 0$ here, we have $k(0) = k$, so $kR(z,q,k)$ is the frequency-domain reflection response to a planar impulse.

Equation (3.10) has a very clear interpretation: to form the reflection response at depth z in the Born approximation, assume the incident impulsive plane wave penetrates without being scattered to each depth z', and is then scattered by the potential $\hat{V}(z',q)$ at that depth. Then use the migration operator $\mathrm{e}^{\mathrm{i}k(q)z}$ to migrate each scattered field back to depth z independently (neglecting all coupling), and superpose the scattered fields due to each $\hat{V}(z',q)$. At the surface $z = 0$ this is clear, but it applies to any depth z.

Note that $\bar{q}(k_x,z,k)$ in (2.16) in the time domain is causal for all z (see figure 2(*b*)) while a time delay/advance $\mathrm{e}^{-\mathrm{i}kz'}$ must be included in (3.10). Also note that $\hat{V}(z',q)$ in (3.10) is scaled by $-\mathrm{i}/(2k(q))$; the reason for this will become apparent in (3.13) below.

Now consider the Born approximation to the layer stripping algorithm (2.14b) and (2.16) applied to (3.10). Taking the Fourier transform (2.4) of (2.8*a*) and using (2.16) gives

$$\bar{q}(z,q,k) = \left(\frac{\partial}{\partial z} + \mathrm{i}k\right) \qquad \bar{p}(z,q,k) = \left(\frac{\partial}{\partial z} + \mathrm{i}k\right)\bar{R}(z,q,k)\mathrm{e}^{\mathrm{i}k(q)z}. \tag{3.11}$$

Inserting (3.10) into (3.11) shows that the Born-approximated layer stripping algorithm computes

$$\bar{q}(z,q,k) = -\mathrm{i}/(2k(q))\hat{V}(z,q)\mathrm{e}^{\mathrm{i}k(q)z} \tag{3.12}$$

from the Born-approximated scattering data. Using (2.14*b*) shows that the Born-approximated layer stripping algorithm computes

$$-2\mathcal{F}_{k\to t}^{-1}\{\bar{q}(z,q,k)\}_{t=z} = \hat{V}(z,q)\mathcal{F}_{k\to t}^{-1}\left\{\frac{\mathrm{e}^{\mathrm{i}k(q)z}}{-\mathrm{i}k(q)}\right\}_{t=z} = \hat{V}(z,q) \tag{3.13}$$

so that it does indeed correctly compute the scattering potential $\hat{V}(z,q)$ in the Born approximation.

4. Numerical results

4.1. Initialization

The algorithm described in section 3 was used to generate the backscattered reflection response $kR(0,q,k)$ to an impulsive plane wave for several different scattering potentials $V(x,z)$. The inverse Fourier transform (2.4) $\partial\check{R}(0,q,t)/\partial t$ of $kR(0,q,k)$ was then used to initialize the discrete layer stripping algorithm of section 2, with (recall $q = k_x$)

$$p(0,t,k_x) = \check{R}(0,q=k_x,t) \qquad q(0,t,k_x) = 2\frac{\partial}{\partial t}\check{R}(0,q=k_x,t). \tag{4.1}$$

The latter initial condition comes from (2.7*a*) and the fact that $\check{R}(z,q,t) = \check{R}(0,q,t+z)$ in the homogeneous overlying half-space $z < 0$, since $R(0,q,t)$ is a *backscattered* (i.e. upward-traveling) wave. Note that the sample applications of section 2 would require different initial conditions.

4.2. Forward problem versus inverse problem algorithms

The invariant imbedding algorithm was used to generate the forward data so that the layer stripping inverse problem algorithm would not simply run the computations of the forward problem algorithm backwards. Although the two algorithms must of course be mathematically equivalent, since they are both 'exact', they are derived from different mathematical principles.

Some specific differences between the forward problem (invariant imbedding) algorithm (FPA) and the inverse problem (layer stripping) algorithm (IPA) are as follows.

(i) The FPA propagates the reflection coefficient at depth $R(c,q,p,k)$. The IPA propagates the field and field gradient $p(z,t,k_x)$ and $q(z,t,k_x)$. Note that $R \neq q/p$, since R is the ratio of downgoing and upgoing *waves*, not field quantities.

(ii) The FPA operates in the k (frequency) domain, while the IPA operates in the t (time) domain.

(iii) The FPA computes $R(c,q,p,k)$ for all c,q,p,k, while the IPA is initialized using $kR(0,q,0,k)$, a slice of the FPA function. Note in the FPA (3.8) the integrals over q' and the differences $q'-q''$; these clearly have no counterpart in the IPA.

(iv) The FPA propagates (3.8), which can be viewed as a 2D generalization of the Riccati equation familiar in 1D inverse scattering. The IPA propagates the coupled system (2.8); note that this differs from the coupled system (3.3) used to derive (3.8).

(v) While both algorithms are discretized in depth, the FBP results did not vary significantly with mesh size, so this should not be an issue. The IBP results also did not vary significantly with mesh size, and gave good results at several different resolutions (see below).

These differences make it clear that errors are not cancelling out algebraically between the FPA and the IPA, i.e., the IPA is not effectively running the FPA computations backwards.

4.3. Summary of results

The numerical performance of the layer stripping algorithm was studied under a variety of conditions. The results may be summarized as follows.

(i) The layer stripping algorithm successfully reconstructed the potential in the absence of noise. The only difficulty was due to the smoothing of the transverse derivative, which slightly smoothed very sharp variations in the lateral direction.

(ii) The layer stripping algorithm continued to work well when a small amount of Gaussian random noise was added to the reflection response. The reconstructed potential was slightly degraded, of course, but the amount of degradation seemed to vary smoothly with the amount of noise—a slight increase in noise level did not vastly degrade the reconstructed potential.

(iii) The layer stripping algorithm reconstructions were superior to those using the Born approximation (as specified in section 2.4 above), in that the Born approximation treated multiple scattering events as additional single scattering events, resulting in errors in the reconstructed potential, particularly for large z. This effect was more pronounced when the potential had numerically large values; for small potentials $V(n\Delta, k\Delta)\Delta \ll 1$ the Born approximation worked quite well. This was as expected; multiple scattering involves products of potentials, and multiplying small values results in even smaller values.

(iv) The performance of the algorithm seemed to vary little with the size of the discretization length Δ, provided that the same Δ was used in the discretized invariant imbedding algorithm. This suggests there may be a close relation between the discretized versions of these algorithms. Coarse grid reconstructions seemed to be merely undersampled versions of the fine grid reconstructions; the basic features of the reconstructions were identical.

We illustrate these points with some numerical examples below. It should be noted that the following is only a representative and illustrative sample of our results; the above conclusions are not based merely on the results below. Unless otherwise specified, all examples used $\Delta = 1/32$, $L = L_x = 1/2$, and $\Delta_k = 1$. The 3D plots are depicting 2D functions $V(x, z)$; they do not represent objects buried in a homogeneous surrounding medium.

4.4. Comparison with the Born approximation

The potential $V(x, z)$ is shown in figure 3(*a*). Note that this is a smooth, rounded potential having compact support in both x and z.

The reconstructed potential using the Born approximation is shown in figure 3(*b*). Although figure 3(*b*) superficially seems to be identical to figure 3(*a*), study carefully the deepest part of the reconstructed $V(x, z)$. The original $V(x, z)$ is zero for $z > 24/32$, while the Born-reconstructed $V(x, z)$ does not become zero until $z > 26/32$; it has a 'tail'. This 'tail' is caused by multiple scattering that is interpreted under the Born approximation as primary scattering due to an additional non-zero portion of the scattering potential; actually, there is no such portion.

The reconstructed potential using the layer stripping algorithm is shown in figure 3(*c*). This reconstruction has no 'tail'; the multiple scattering that produces it has been accounted for in the algorithm and eliminated. The reconstruction is almost perfect.

A different potential is shown in figure 4(*a*). Note that this potential function is constant over a central 'plateau', and then drops off rapidly to zero.

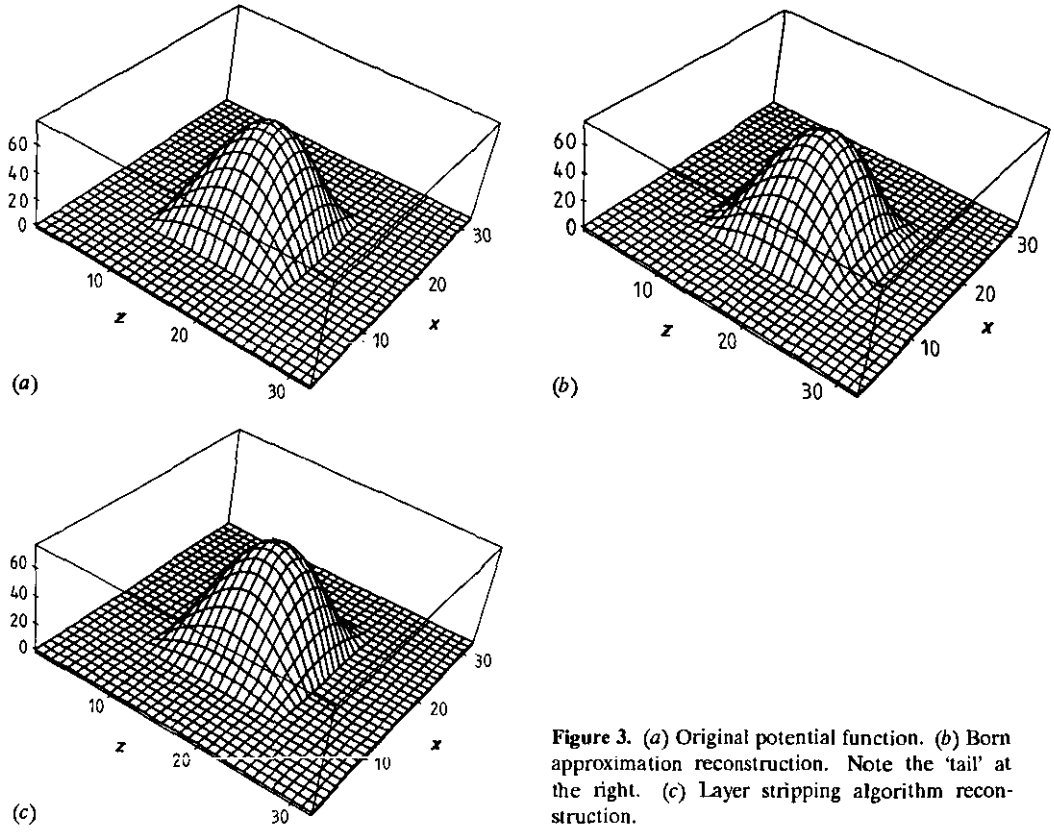

Figure 3. (*a*) Original potential function. (*b*) Born approximation reconstruction. Note the 'tail' at the right. (*c*) Layer stripping algorithm reconstruction.

The reconstructed potential using the Born approximation is shown in figure 4(*b*). Note again the presence of a 'tail' at its deepest part, while there is no 'tail' at its shallowest part, since multiple scattering has not yet had *time* to occur in this part of the time-domain impulse response (the lack of symmetry in z is apparent if one looks at the figure as a whole). Also note the problems in reconstructing the lateral edges of the potential function; the central 'plateau' is much smaller than it should be.

The reconstructed potential using the layer stripping algorithm is shown in figure 4(*c*). Again the 'tail' caused by multiple scattering has been eliminated. However, the shallowest and deepest edges of the 'plateau' have been rounded off slightly. Since this is symmetric between the shallowest and deepest parts, it is not due to multiple scattering. We attribute it to smoothing in the transverse derivative.

4.5. Effects of additive noise

The potential $V(x, z)$ used in figure 3 was scaled as shown in figure 5(*a*), and Gaussian random noise was added to the reflection response $R(0, q, k)$. The signal-to-noise ratio, computed as the square root of the sum of the squares of the discrete signal values divided by the square root of the sum of the squares of the discrete noise values, was found to be 36 dB for one run and 18 dB for another (to get power SNR these values should be doubled). Note that any powers of Δ and numbers of points being averaged will cancel in this ratio.

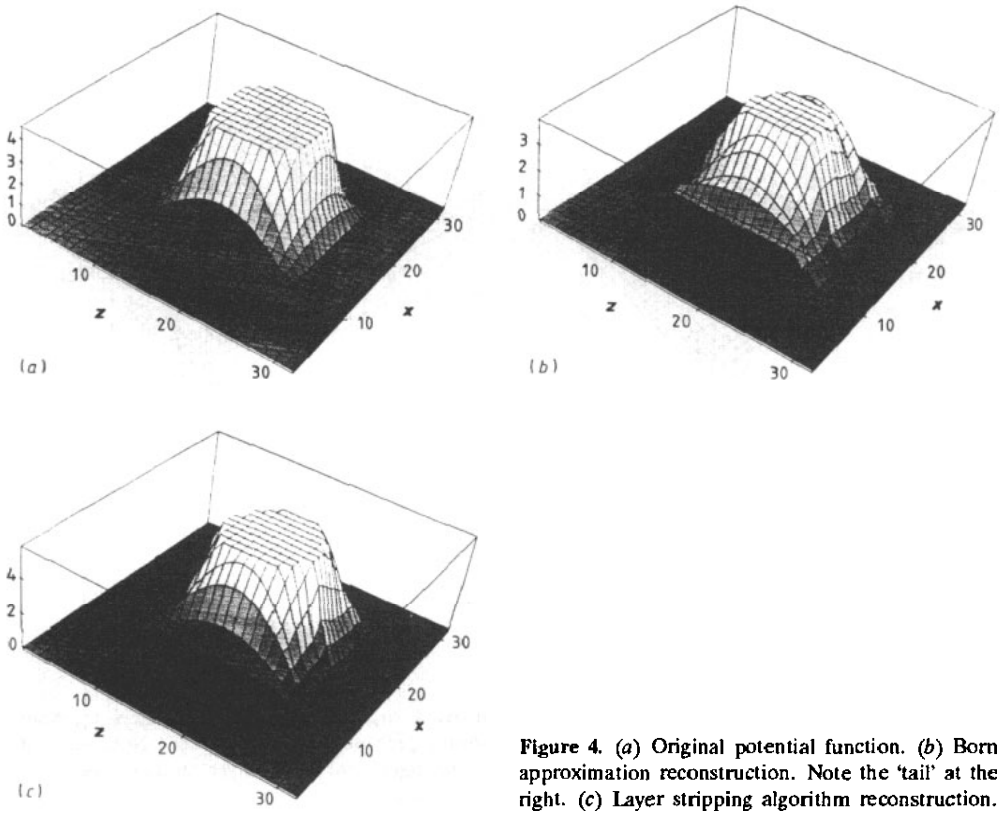

Figure 4. (*a*) Original potential function. (*b*) Born approximation reconstruction. Note the 'tail' at the right. (*c*) Layer stripping algorithm reconstruction.

The reconstructions at 36 dB are virtually perfect; in fact, the reconstructions shown in figure 3 are actually these reconstructions. The reconstructions at 18 dB are shown in figure 5(*b*) using the Born approximation and figure 5(*c*) using the layer stripping algorithm. Note that even in these noisy reconstructions the 'tail' is still a significant feature in the Born approximation reconstruction, while the layer stripping reconstruction has correctly removed the 'tail'.

To see the degradation of the layer stripping algorithm in the presence of increasing amounts of noise added to the reflection response, study figure 6. Figure 6(*a*) shows the original potential function, which is the same as figure 4(*a*). Figure 6(*b*) shows a noisy reconstruction of the potential function shown in figure 6(*a*), and in figure 6(*c*) the signal-to-noise ratio has been reduced by a factor of four. The increasing degradation of the reconstruction is obvious, but the layer stripping algorithm does not fall apart even in large amounts of additive noise.

A similar study is carried out for a different potential function in figure 7. Figure 7(*a*) shows the original potential function, and figures 7(*b*) and 7(*c*) correspond to figures 6(*b*) and 6(*c*). The only notable feature of the layer stripping reconstructions is the slight (one pixel wide) 'shelf' induced by the smoothed transverse derivative (this is discussed in more detail below); otherwise, the reconstructed potential smoothly degrades with increasing noise.

Note the presence of the sharp ridge along the line $z = 0$ in figures 6 and 7. This ridge is due to the non-zero mean of the noise being added to $R(0, q, k)$. When

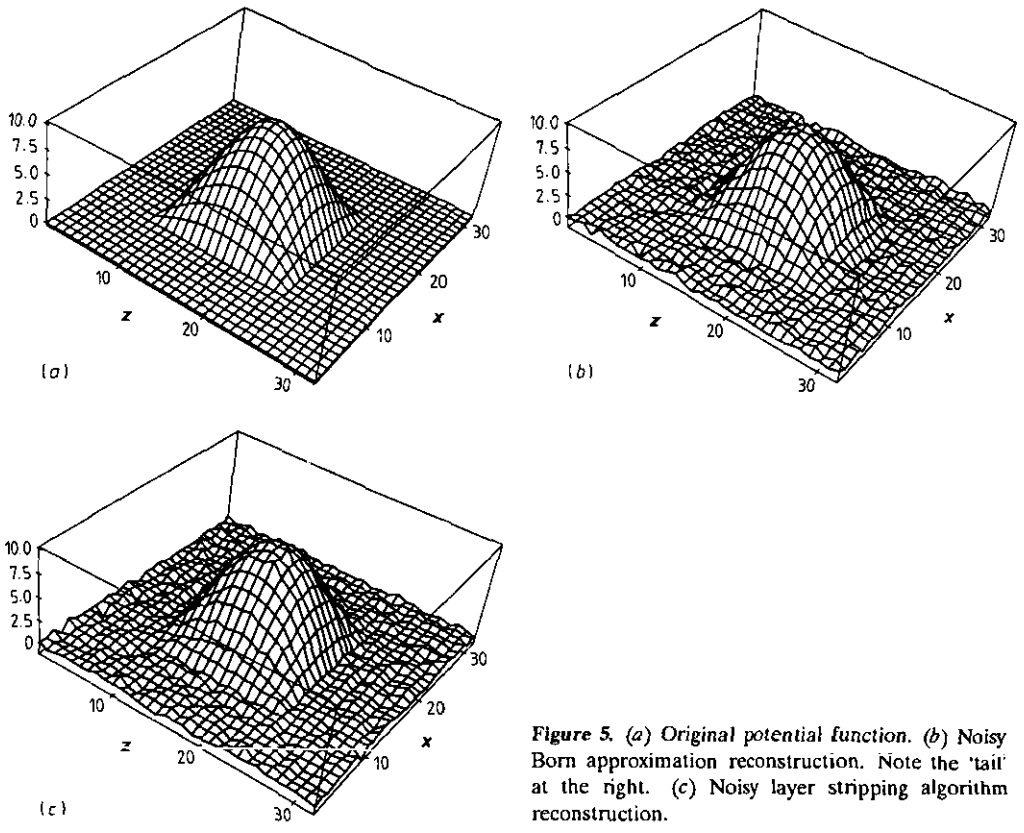

Figure 5. (*a*) *Original potential function.* (*b*) Noisy Born approximation reconstruction. Note the 'tail' at the right. (*c*) Noisy layer stripping algorithm reconstruction.

$V(x, z)$ is computed by taking the inverse Fourier transform (2.9), this non-zero mean, a constant in the Fourier wavenumber k domain, becomes an impulse in the spatial z domain. This impulse is the ridge.

4.6. Discussion of numerical stability with noise

The smooth degradation of the reconstructed potential with increasing noise levels might seem surprising, since the inverse scattering problem is known to be ill-conditioned. The reason for this is that multiple scattering has a relatively small (compared to single scattering) effect, so that the Born approximation result will be approximately the same as the layer stripping result. The Born approximation is linear, so that any noise added to the reflection response will produce an addition to the reconstructed potential whose strength is directly proportional to the noise strength (halving the noise will halve the addition); hence the Born-reconstructed potential will degrade smoothly, and it is not surprising that the reconstructed potential from layer stripping also degrades smoothly.

This heuristic argument should not be taken too far; in the 1D case, it is well known that large noise levels can cause severe problems in layer stripping algorithms, and indeed in *any* 'exact' method. The reason for this is *not* numerical instability, as is commonly believed; the 1D layer stripping algorithm is identical to the Schur algorithm (see [8]), which is *known to be numerically stable.*

The reason that 1D layer stripping algorithms can give unstable results when they

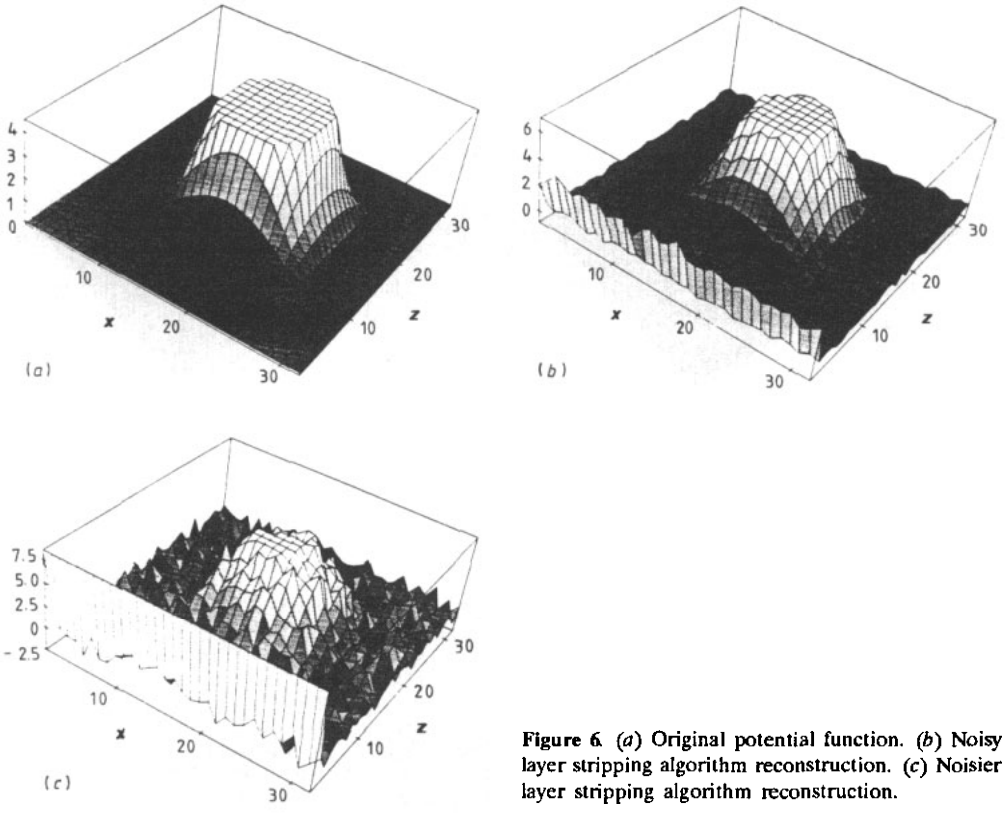

Figure 6. (*a*) Original potential function. (*b*) Noisy layer stripping algorithm reconstruction. (*c*) Noisier layer stripping algorithm reconstruction.

are applied to noisy reflection data is as follows. It is well known that the free-surface reflection response of a 1D layered medium to an impulsive plane wave below the surface is one side of the autocorrelation of its transmission response; hence it must be positive semi-definite. Noise added to the reflection response can make the two-sided response (the reflection response added to its time reversal) become non-positive semi-definite, in which case it is no longer the reflection response to *any* layered medium. The problem is now ill-posed, in the sense of having no solution; it is not surprising that the layer stripping algorithms become unstable.

However, small amounts of additive noise will not cause the reflection response to become non-positive semi-definite; as long as this is true, the layer stripping algorithms will behave well numerically. Our results in this paper suggest that a a similar situation is present in the 2D inverse scattering problem considered here; this is a topic of current research.

4.7. Smoothed reconstructions due to smoothed transverse derivative

The smoothing in the transverse derivative incurred by using the clipped filter (2.10) causes a slight but noticeable smoothing of $V(x, z)$ along the x direction. This was manifested in the reconstructions in figure 7 by the 'shelf' that appeared at the ends of the reconstructed potential function. Another example of this is illustrated in figure 8. Figure 8(*a*) shows the original potential function, which was produced by taking the potential function of figure 7(*a*) and adding random noise to it. The

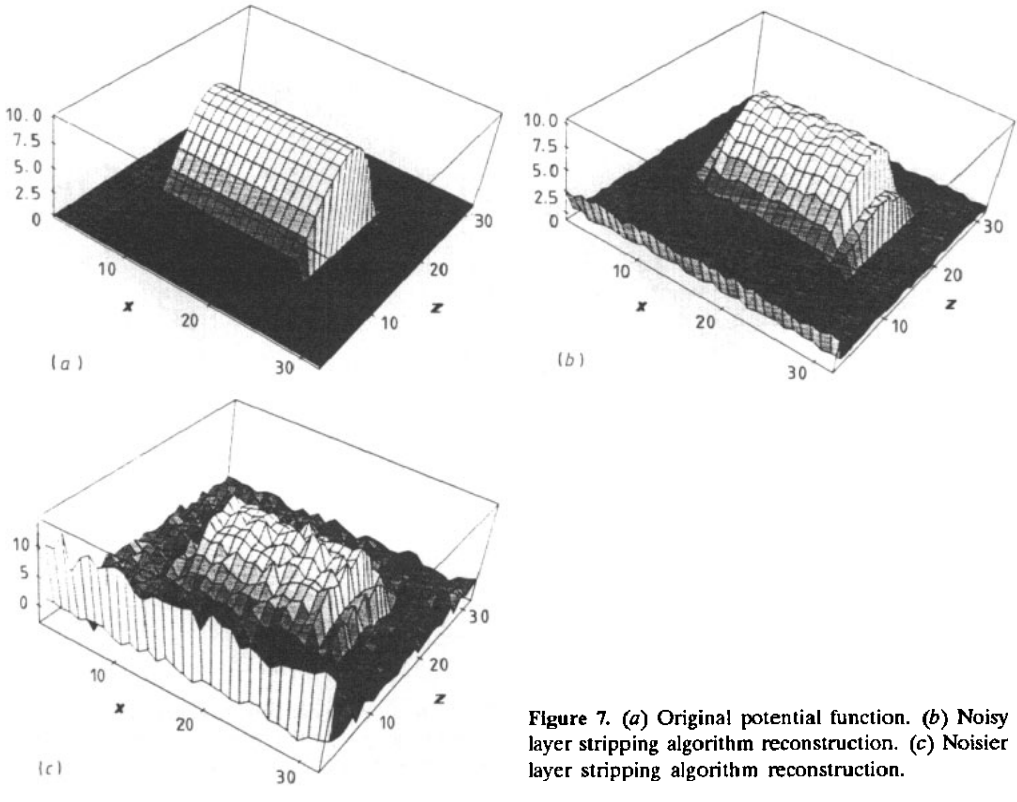

Figure 7. (*a*) Original potential function. (*b*) Noisy layer stripping algorithm reconstruction. (*c*) Noisier layer stripping algorithm reconstruction.

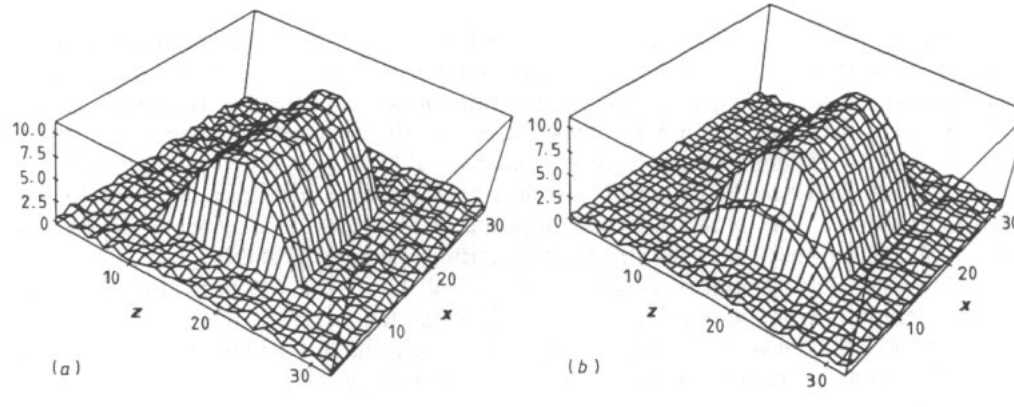

Figure 8. (*a*) Original 'noisy' potential function. (*b*) Layer stripping algorithm reconstruction.

idea here is that in real life potential functions will not have simple analytic forms; they will be complicated functions. Hence figure 8(*a*) is closer to a realistic potential function.

The reconstructed potential from the layer stripping algorithm is shown in figure 8(*b*). Note again the one-pixel-wide 'shelf' at each of the two flat ends of the potential function. We attribute this to the smoothing of the transverse derivative in

the layer stripping algorithm; unable to reconstruct the sharp jump from zero, the algorithm provides a laterally smoothed reconstruction in which the reconstructed potential takes two smaller lateral jumps instead of a single large jump. Note that the 'shelf' is half the height of the jump in x at each depth z.

Also note in figure 8(b) that the 'noisy' part of the potential in figure 8(a) has been noticeably smoothed. This again seems to be due to the smoothing in the transverse derivative; note that the reconstructed potential is 'rougher' in the z direction (for which there is no smoothing) than in the x direction (in which there is smoothing). This smoothing effect should be taken into consideration in potentials reconstructed using layer stripping algorithms.

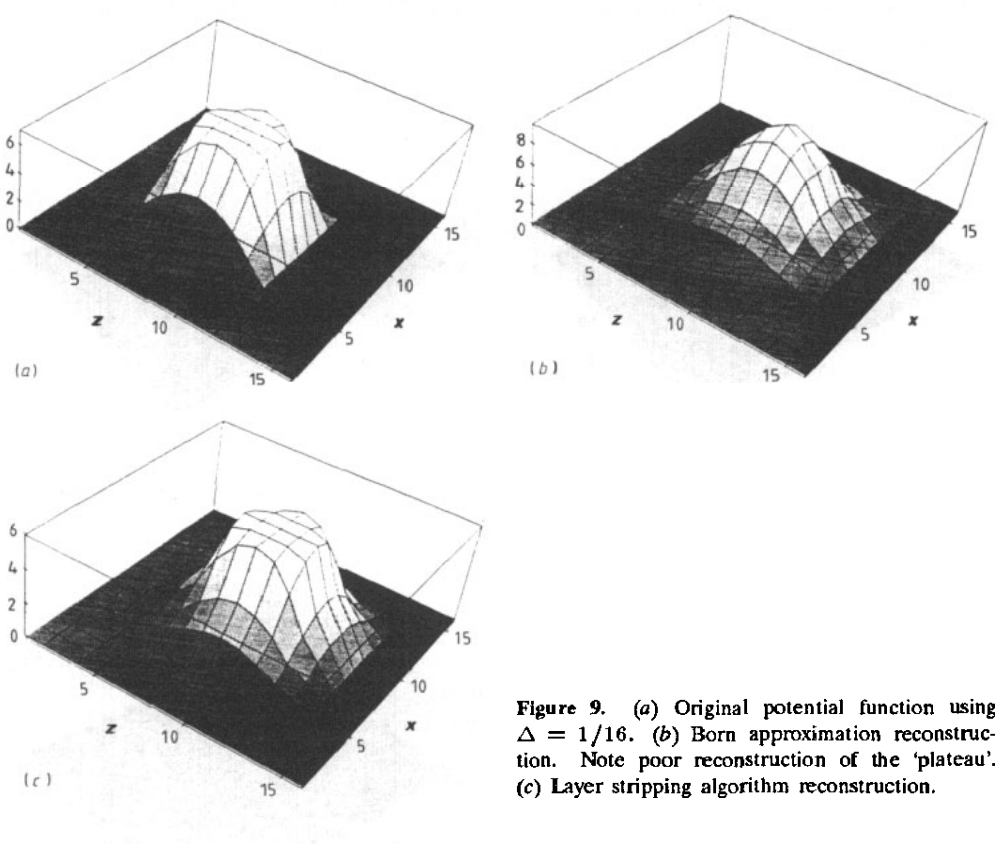

Figure 9. (a) Original potential function using $\Delta = 1/16$. (b) Born approximation reconstruction. Note poor reconstruction of the 'plateau'. (c) Layer stripping algorithm reconstruction.

4.8. Effect of discretization length Δ

The above numerical runs all used $\Delta = 1/32$. Results for a larger $\Delta = 1/16$ are shown in figure 9. Figure 9(a) shows the original potential, which is an undersampled version of the potential in figure 4(a). The reconstructed potential using the Born approximation is shown in figure 9(b). Note how poorly the Born approximation reconstructs the central 'plateau' of the potential function. The reconstructed potential using the layer stripping algorithm is shown in figure 9(c). Although the central 'plateau' is reconstructed quite well, the potential function as a whole is spread out one pixel in each direction. This shows that while the invariant imbedding and

layer stripping algorithms are clearly closely connected, the discretized layer stripping algorithm is *not* merely running the invariant imbedding algorithm backwards.

Results for a smaller $\Delta = 1/64$ are shown in figure 10. Figure 10(a) shows the original potential, which is a more finely sampled version of the potential in figure 4(a). The reconstructed potential using the layer stripping algorithm is shown in figure 10(b). The reconstruction is almost perfect—even the lateral smoothing caused by the smoothed transverse derivative is not apparent. This is due to the fact that although $\Delta_k = 1$, the maximum value of k_x is now 32 instead of 16; the smoothing starts at a much higher wavenumber. A very close comparison of figures 10(a) and 10(b) show that the reconstruction is not quite perfect; the reconstructed potential is still spread out one pixel in each direction. But this effect is virtually negligible on this scale.

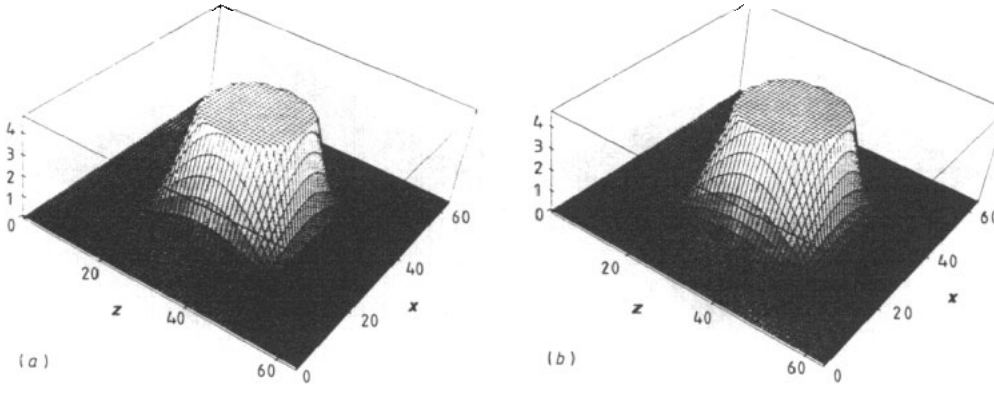

Figure 10. (a) Original potential function using $\Delta = 1/64$. (b) Layer stripping algorithm reconstruction.

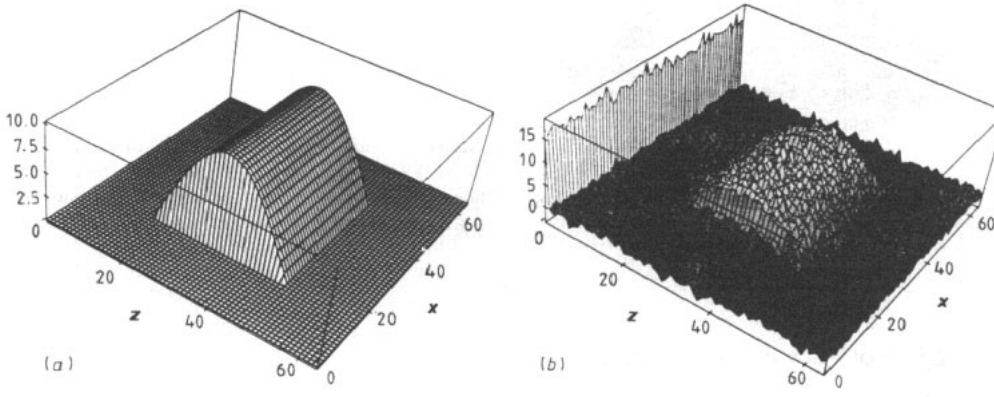

Figure 11. (a) Original potential function using $\Delta = 1/64$. (b) Noisy layer stripping algorithm reconstruction.

One final example combines a smaller Δ, additive noise in the reflection response, and smoothed reconstruction. Figure 11(a) shows the original potential, which is a more finely sampled version of the potential in figure 7(a). Random noise was added to the reflection data, at a signal-to-noise ratio of 15.7 dB. The reconstructed potential

using the layer stripping algorithm is shown in figure 11(*b*). All the features discussed in section 4.3 are again present in figure 11(*b*). These include the 'shelf', still one pixel wide, the ridge along the line $z = 0$, and the main shape of the potential function still visible in the noise. This shows that these effects occur at different discretization lengths, and indeed may be endemic to layer stripping reconstructions with noise for any Δ.

5. Conclusion

The numerical performance of the 2D layer stripping algorithm of [4] has been studied for the first time. This represents the first numerical implementation of an 'exact' non-iterative inverse scattering algorithm that includes the effects of *all* multiple scattering and diffraction effects. The forward scattering data were generated using the invariant imbedding algorithm of [5]. The results indicated that layer stripping is a viable technique for solving 2D Schrödinger equation inverse potential problems, for which two applications were briefly reviewed.

Two particularly important results were that: (1) the 'exact' reconstructions using the layer stripping algorithm are a noticeable improvement over the Born approximation reconstructions; and (2) small amounts of additive noise in the reflection response do not cause numerical instability in the layer stripping algorithm. The results were illustrated using several numerical examples. It was also shown for the first time that the Born approximation to the layer stripping algorithm reconstructs the scattering potential from the reflection response generated by the Born approximation to the invariant imbedding algorithm of [5].

Acknowledgments

It is a pleasure to acknowledge the help of Ms Susan Wei, who helped with the preliminary stages of this research. This research was supported by the Office of Naval Research under grant # N00014-90-J-1897.

References

[1] Coen S, Cheney M and Weglein A 1984 Velocity and density of a two dimensional acoustic medium from point source surface data *J. Math. Phys.* **25** 1857–60

[2] Yagle A E 1987 A layer stripping fast algorithm for the two-dimensional direct current inverse resistivity problem *IEEE Trans. Geosci. Rem. Sensing* **GE-25** 558–63

[3] Cheney M 1984 Inverse scattering in dimension two *J. Math. Phys.* **25** 94–102

[4] Yagle A E and Levy B C 1986 Layer stripping solutions of multidimensional inverse scattering problems *J. Math. Phys.* **27** 1701–10

[5] Wilcox R 1970 Wave propagation through longitudinally and transversally inhomogeneous slabs—I *Invariant Imbedding* ed R E Bellman and E D Denman (New York: Springer)

[6] Cheney M 1990 Stability analysis of the Yagle–Levy multidimensional inverse scattering algorithm *Preprint* Department of Mathematical Sciences, Rensselaer Polytechnic Institute, Troy, NY

[7] Snieder R 1990 The role of the Born approximation in nonlinear inversion *Inverse Problems* **6** 247–66

[8] Bruckstein A M, Levy B C and Kailath T 1985 Differential methods in inverse scattering *SIAM J. Appl. Math.* **45** 312–35